PRAMANA — journal of physics

© Indian Academy of Sciences

Vol. 81, No. 2
August 2013
pp. 189–202

Generalized Freud's equation and level densities with polynomial potential

AKSHAT BOOBNA* and SAUGATA GHOSH
The Creative School, E-791, C.R. Park, New Delhi 110 017, India
*Corresponding author. E-mail: akshatb42@gmail.com

MS received 14 December 2012; revised 28 March 2013; accepted 17 April 2013

Abstract. Orthogonal polynomials with weight $\exp[-NV(x)]$ are studied where $V(x) = \sum_{k=1}^{d} a_{2k}x^{2k}/2k$ is a polynomial of order $2d$. The generalized Freud's equations for $d = 3$, 4 and 5 are derived and using this $R_\mu = h_\mu/h_{\mu-1}$ is obtained, where h_μ is the normalization constant for the corresponding orthogonal polynomials. Moments of the density functions, expressed in terms of R_μ, are obtained using Freud's equation and using this, explicit results of level densities as $N \to \infty$ are derived using the method of resolvents. The results are compared with those using Dyson–Mehta method.

Keywords. Orthogonal polynomial; Freud's equation; Dyson–Mehta method; methods of resolvents; level density.

PACS Nos 02.30.Gp; 05.45.Mt

1. Introduction

Universality in random matrix theory [1–4] has led people to study orthogonal [5–7] and skew-orthogonal polynomials [8] in great detail. However, in the process, the non-universal level densities are neglected in spite of the possibility of its direct application in various physical systems. In this context, we study level densities of a class of non-Gaussian random matrix ensembles and thereby develop the theory of orthogonal polynomials.

Orthogonal polynomials are defined as

$$\int_{\mathbb{R}} P_n(x)P_m(x)w(x)\mathrm{d}x = h_n\delta_{nm}, \quad n, m \in \mathbb{N}. \tag{1.1}$$

We study orthogonal polynomials with weight function $w(x) = \exp(-NV(x))$, where

$$V(x) = \sum_{k=1}^{d} a_{2k}x^{2k}/(2k), \quad a_{2d} > 0. \tag{1.2}$$

DOI: 10.1007/s12043-013-0563-y; *e*Publication: 31 July 2013

Here, we make a numerical analysis of orthogonal polynomials corresponding to $d = 3$, 4 and 5. We derive the corresponding Freud's equation and calculate $R_\mu = h_\mu/h_{\mu-1}$. We observe interesting patterns in the behaviour of R_μ.

Once we have an understanding of R_μ, we use these results to obtain level densities of non-Gaussian ensembles of random matrices. We know that variation of the first n eigenvalues of a random matrix can be studied by the n-point correlation function, $R_n^{(\beta)}(x_1, ..., x_n)$ which is defined by

$$R_n^{(\beta)}(x_1, ..., x_n) = \frac{N!}{(N-n)!} \int_{\mathbb{R}^{N-n}} \mathrm{d}x_{n+1} ... \mathrm{d}x_N \, P_{\beta,N}(x_1, ..., x_N), \tag{1.3}$$

where $\beta = 1, 2, 4$ correspond to ensembles of random matrices invariant under orthogonal, unitary and symplectic transformations. This allows us to find the probability density of the n eigenvalues at $x_1, ..., x_n$, irrespective of the eigenvalues at $x_{n+1}, ..., x_N$. From here, using the Mehta–Dyson formula, we can calculate the level density, $R_1^{(\beta)}(x)$, which, for $\beta = 2$ can be written as [9–12]

$$R_1^{(2)}(x) = \sum_{\mu=0}^{N-1} (h_\mu)^{-1} [P_\mu(x)]^2 \mathrm{e}^{-NV(x)}. \tag{1.4}$$

To calculate $R_1^{(2)}(x)$ as $N \to \infty$, the standard method is to use the Christoffel–Darboux formula and the asymptotic results of orthogonal polynomials. The latter is not always available for general polynomial potential in spite of some serious contributions from Nevai [13]. However, more rigorous results have been obtained recently by several authors [6,14–17] on the asymptotics of orthogonal polynomials with $V(x) = x^{2d}$ using the Riemann–Hilbert technique.

In this paper, we use the method of resolvent to obtain the level densities as $N \to \infty$. This needs an understanding of moments M_k defined as

$$M_k = \int_{\mathbb{R}} x^k R_1^{(2)}(x) \mathrm{d}x, \quad k \in \mathbb{N}. \tag{1.5}$$

This is derived using the values of R_μ using generalized Freud's equation, which we derive independently. Using this, we obtain the corresponding level densities. This gives us a good understanding of the origin of multiple band formation in the level densities in polynomial potential.

Finally, we compare these results with that obtained numerically from the Dyson–Mehta method which is cumbersome and has its limitations for even reasonable values of N.

The paper is organized as follows: In §2, we study the $d = 3$ case and observe the behaviour of R_μ for different values of a_k. Sections 3 and 4 deal with $d = 4$ and $d = 5$ results. Section 5 contains our concluding remarks.

2. $d = 3$ Case

2.1 *Freud's equation*

Orthogonal monic polynomials with even weights satisfy a recursion relation [5]

$$xP_\mu = P_{\mu+1} + R_\mu P_{\mu-1}, \quad \mu \in \mathbb{N}, \tag{2.1}$$

where $R_\mu = h_\mu/h_{\mu-1}$, for $\mu \geq 1$ and $R_0 = 0$.

A major development in the study of quartic weight ($d = 2$ in eq. (1.2)) polynomials [18–20] was the following recursive equation in R_μ due to [21]:

$$\mu + 1 = NR_{\mu+1}[a_4(R_{\mu+2} + R_{\mu+1} + R_\mu) + a_2]. \tag{2.2}$$

Now, we derive a similar Freud's equation for sextic potential, i.e. $d = 3$ in eq. (1.2). We use the identity

$$\int \mathrm{d}x[P_{\mu+1}(x)P_\mu(x)\mathrm{e}^{-NV(x)}]' = 0. \tag{2.3}$$

Using $P_\mu(x) = x^\mu + \cdots$ and the orthonormality condition (1.1), we get

$$\int [\mathrm{e}^{-NV(x)}][P'_{\mu+1}(x)P_\mu(x) + P_{\mu+1}(x)P'_\mu]\mathrm{d}x$$
$$+ \int N[a_6x^5 + a_4x^3 + a_2x]P_{\mu+1}(x)P_\mu(x)\mathrm{e}^{-NV(x)}]\mathrm{d}x = 0.$$

This gives us

$$\begin{aligned}(\mu+1)h_\mu = &\int Na_6x^5P_{\mu+1}(x)P_\mu(x)\mathrm{e}^{-NV(x)}\mathrm{d}x\\ &+\int Na_4x^3P_{\mu+1}(x)P_\mu(x)\mathrm{e}^{-NV(x)}\mathrm{d}x\\ &+\int Na_2xP_{\mu+1}(x)P_\mu(x)\mathrm{e}^{-NV(x)}\mathrm{d}x.\end{aligned}$$

Using (2.1), we obtain

$$\begin{aligned}\mu+1 = {} & NR_{\mu+1}[a_6(R_{\mu+2}(R_\mu + R_{\mu+1} + R_{\mu+2} + R_{\mu+3})\\ &+ R_{\mu+1}(R_\mu + R_{\mu+1} + R_{\mu+2})\\ &+ R_\mu(R_{\mu-1} + R_\mu + R_{\mu+1}))\\ &+ a_4(R_{\mu-1} + R_\mu + R_{\mu+1}) + a_2].\end{aligned} \tag{2.4}$$

Here we note that the corresponding Freud's equation is cubic in nature thereby giving rise to oscillatory behaviour.

2.2 *The R_μ plot*

For the $d = 2$ case, two main features were observed in the R_μ plot from the original Freud's equation: A two-band structure formed by an oscillation between two values, converging to a single band.

In the sextic case, the two-band and single band structures reappear. However a new, more chaotic structure is also seen, appearing either between one-band and one-band or one-band and two-band structures. Henceforth, it is termed as a 'transient structure'.

2.2.1 *Single-band structure.* For the single-band structure, all the terms in the Freud's equation are equal. Thus, we obtain a λ-dependent cubic equation (where $\lambda = \mu/N$), solving which we obtain one real solution

$$D_{\pm} = \frac{27}{2}(2a_4^3 - 10a_6a_4 - 100a_6^2\lambda) \pm\sqrt{(2a_4^3 - 10a_6a_4 - 100a_6^2\lambda)^2 - 4(a_6^2 - (10a_6a_2/3))^3}, \tag{2.5}$$

$$R_\mu = -\frac{a_4}{10a_6} - \frac{\sqrt[3]{D_+}}{30a_6} - \frac{\sqrt[3]{D_-}}{30a_6}, \tag{2.6}$$

which gives the value of R_μ for λ values where single band exists.

2.2.2 *Two-band structure.* Solving the Freud's equation assuming that two bands are formed (as seen), i.e., $A_0 = R_0 = R_2 = R_4 = \cdots$, $A_1 = R_1 = R_3 = R_5 = \cdots$, for $N \gg \mu$, we get

$$A_0 + A_1 = \frac{-a_4 + \sqrt{a_4^2 - 4a_2a_6}}{2a_6}. \tag{2.7}$$

It has been numerically verified that the bottom band (A1) tends to 0, and we find that $A_1 \propto 1/N$ and $A_1 \propto 1/(a_4)^2$.

2.2.3 *Transient structure.* When the transient structure is divided modulo 3 into three bands (b_0, b_1 and b_2 in figure 1), it is seen that each of the three separate bands continuously oscillates, and converges to a common value.

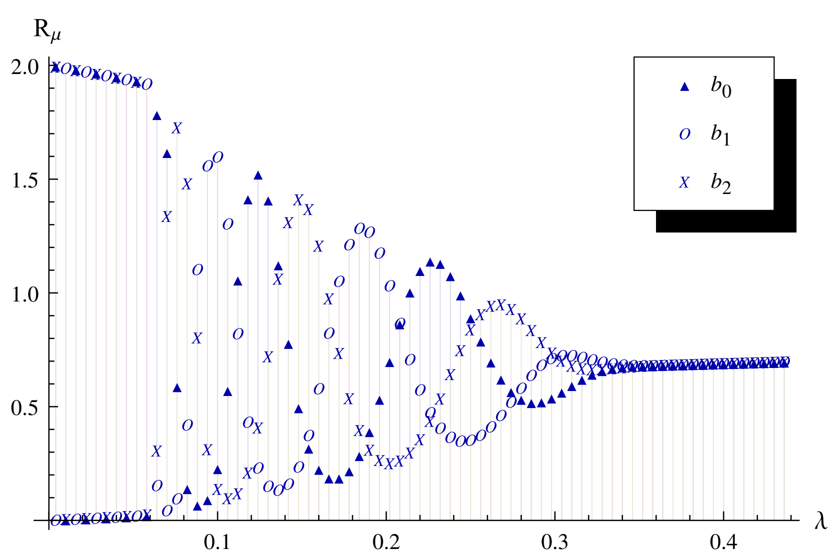

Figure 1. R_μ plot modulo 3 for $d = 3$, $a_6 = 1$, $a_4 = -2.5$, $a_2 = 1$, $N = 500$ using eq. (2.4).

The sum mod 3 for the duration of the transient structure oscillates above the value

$$b_0 + b_1 + b_2 \approx \frac{-a_4 + \sqrt{a_4^2 - 4a_2a_6}}{2a_6}, \tag{2.8}$$

where b_0, b_1 and b_2 correspond to three consecutive values from each of the bands.

2.3 *Critical a_4s*

On analysing the roots of the sextic potential, we obtain the critical value of a_4, denoted here by $a_{4\mathrm{c}}$, where the structure of the R_μ plot changes. We find the points at which potential plot touches 0, and obtain

$$a_{4\mathrm{c}} = -\sqrt{\frac{48}{9}a_2a_6}. \tag{2.9}$$

In the R_μ plot, when $a_4 < a_{4\mathrm{c}}$, we observe a two-band structure, followed by a transient structure, which converges to single band and when $a_4 > a_{4\mathrm{c}}$, we see a one-band structure, followed by a transient structure, which converges to single band.

We now analyse the behaviour of R_μ as a_4 approaches $a_{4\mathrm{c}}$ (figure 2). It is observed the transient structure resolves into three distinct bands near $a_{4\mathrm{c}}$. Exactly at the critical value, two of these bands coincide to form an upper band, and the third band forms a lower band, creating a pseudo-two-band structure.

2.4 *Level density*

In this subsection, we derive the level density using the method of resolvent [8,22,23] as $N \to \infty$. The result is expressed in terms of moments M_k (1.5) which are derived using the results from the Freud's equation. We then compare the result with the level density for $N = 30$ using (1.4). For $d = 3$, we have chosen the coefficients so that we get multiple bands in the level density.

From the definition of $\partial P_{\beta,N}(x_1, \ldots, x_N)$, we have

$$\frac{\partial P_{\beta,N}(x_1, \ldots, x_N)}{\partial x_1} = \left(\beta \sum_{j \neq 1} \frac{1}{x_1 - x_j} + \frac{w'(x_1)}{w(x_1)}\right) P_{\beta,N}(x_1, \ldots, x_N). \tag{2.10}$$

We note that from here on, $\beta = 2$ and we shall not explicitly write it. For $n = 1$, we have

$$\frac{\partial R_1(x)}{\partial x_1} = \beta \int \frac{R_2(x, y)}{x - y} \mathrm{d}y + \frac{w'(x_1)}{w(x_1)} R_1(x). \tag{2.11}$$

For large N, the integral on the right can be replaced by a principal-value integral involving $R_2(x, y) \approx R_1(x)R_1(y)$. Further, $\partial R_1(x)/\partial x$ can be dropped. This follows from the behaviour of $R_1(x)$ and $R_2(x, y)$ for large N.

$$\beta R_1(x) \int \frac{R_1(y)}{x - y} \mathrm{d}y + \frac{w'(x)}{w(x)} R_1(x) = 0. \tag{2.12}$$

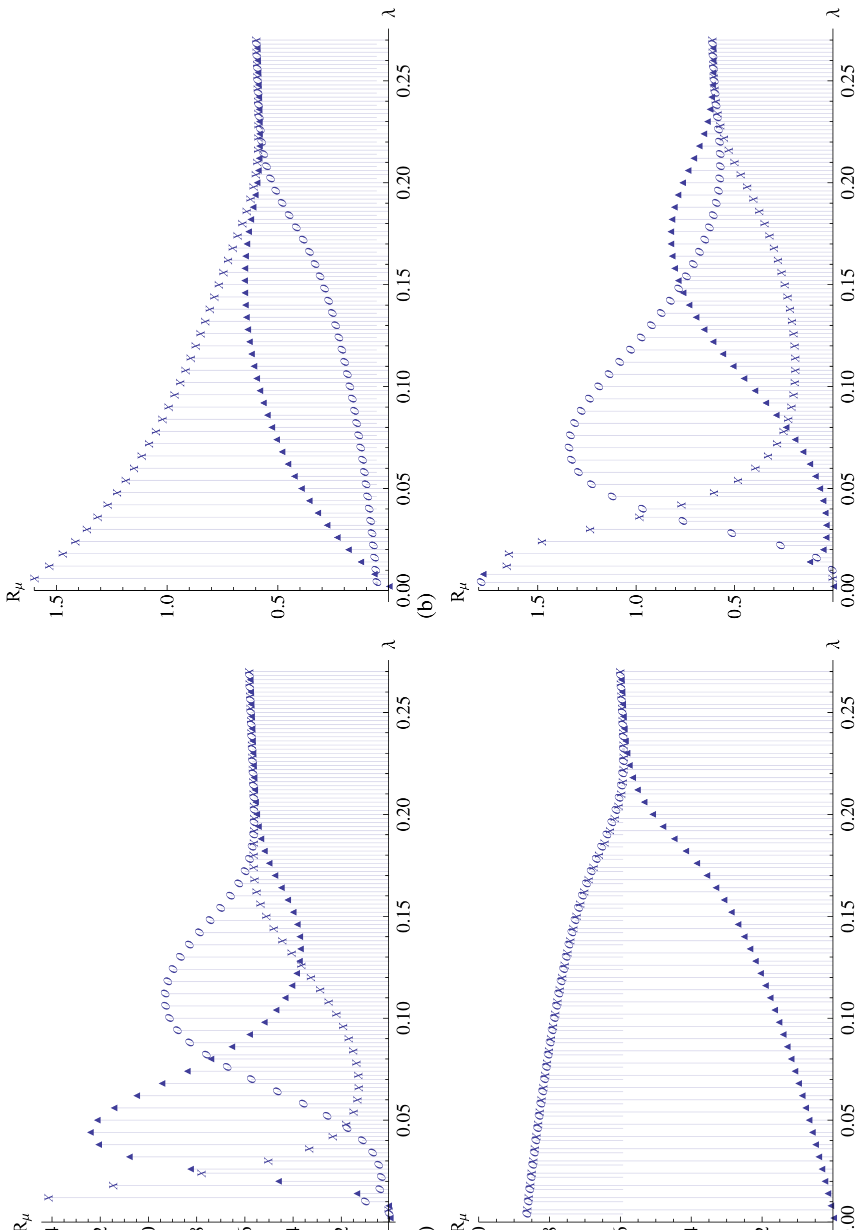

Figure 2. R_μ plot as a_4 approaches a_{4c} for $a_6 = 1$, $a_2 = 1$, $N = 500$. **(a)** $a_4 = -2.25$, **(b)** $a_4 = -2.30$, **(c)** $a_4 = -\sqrt{48/9}$ $(= a_{4c})$ and **(d)** $a_4 = -2.35$.

We use the resolvent $G(z)$ to solve the integral equation.

$$G(z) = \int \frac{R_1(y)}{z-y}\mathrm{d}y. \tag{2.13}$$

Thus we have from (2.12),

$$\begin{aligned} 0 &= -N\int_{-\infty}^{\infty}\frac{V'(x)R_1(x)}{z-x}\mathrm{d}x + \int_{-\infty}^{\infty}\mathrm{d}x\frac{R_1(x)}{z-x}\int_{-\infty}^{\infty}\mathrm{d}y\frac{R_1(y)}{x-y} \\ &= \frac{1}{2}\int_{-\infty}^{\infty}\int_{-\infty}^{\infty}\frac{R_1(x)R_1(y)}{x-y}\left[\frac{1}{z-x}-\frac{1}{z-y}\right]\mathrm{d}x\mathrm{d}y - NV'(z)G(z) \\ &\quad + N\int_{-\infty}^{\infty}\frac{V'(z)-V'(x)}{z-x}R_1(x)\mathrm{d}x \end{aligned} \tag{2.14}$$

implying

$$G^2(z) - 2NV'(z)G(z) + 2N\int_{-\infty}^{\infty}\frac{V'(z)-V'(x)}{z-x}R_1(x)\mathrm{d}x = 0. \tag{2.15}$$

Here, we recall [8] that we use the scaling $V(x) \to V(x)/2$ to obtain the corresponding results. Finally,

$$\begin{aligned} [\pi R_1(x)]^2 &= N\int_{-\infty}^{\infty}\frac{V'(z)-V'(x)}{z-x}R_1(x)\mathrm{d}x - N^2\left[\frac{V'(x)}{2}\right]^2 \\ &= N\left[a_6(x^4N + x^2M_2 + M_4) + a_4(x^2N + M_2) + a_2N\right] \\ &\quad - N^2x^2\left(\frac{a_6x^4 + a_4x^2 + a_2}{2}\right)^2 \end{aligned}$$

$$\begin{aligned} \left[\frac{\pi R_1^{(2)}(x)}{N}\right]^2 &= \left(\frac{a_6M_4 + a_4M_2}{N} + a_2\right) \\ &\quad + x^2\left[\left(a_6x^2 + \frac{a_6M_2}{N} + a_4\right)\right. \\ &\quad \left. -\frac{1}{4}\left(a_6x^4 + a_4x^2 + a_2\right)^2\right]. \end{aligned} \tag{2.16}$$

Now that we have derived $R_1^{(2)}(x)$ in terms of M_2 and M_4, we would be interested to calculate them using Freud's equation. We use

$$\begin{aligned} M_k &= \sum_{\mu}\int\frac{x^kP_{\mu}^2(x)}{h_{\mu}}w(x)\mathrm{d}x \\ &= \sum_{\mu}\int\frac{(x^kP_{\mu}(x))P_{\mu}(x)}{h_{\mu}}w(x)\mathrm{d}x \\ &= \sum_{\mu}\sum_{\nu}\int\frac{C_{\nu}P_{\nu}(x)P_{\mu}(x)}{h_{\mu}}w(x)\mathrm{d}x \\ &= \sum_{\mu}C_{\mu}, \end{aligned} \tag{2.17}$$

where C_μ are coefficients which can be expressed in terms of R_μ. A few typical examples are

$$M_2 = \sum_{\mu=0}^{N-1} \left(R_{\mu+1} + R_\mu\right), \tag{2.18}$$

$$M_4 = \sum_{\mu=0}^{N} \left(R_\mu^2 + R_{\mu+1}^2 + 2R_\mu R_{\mu+1} + R_{\mu+1}R_{\mu+2} + R_\mu R_{\mu-1}\right), \tag{2.19}$$

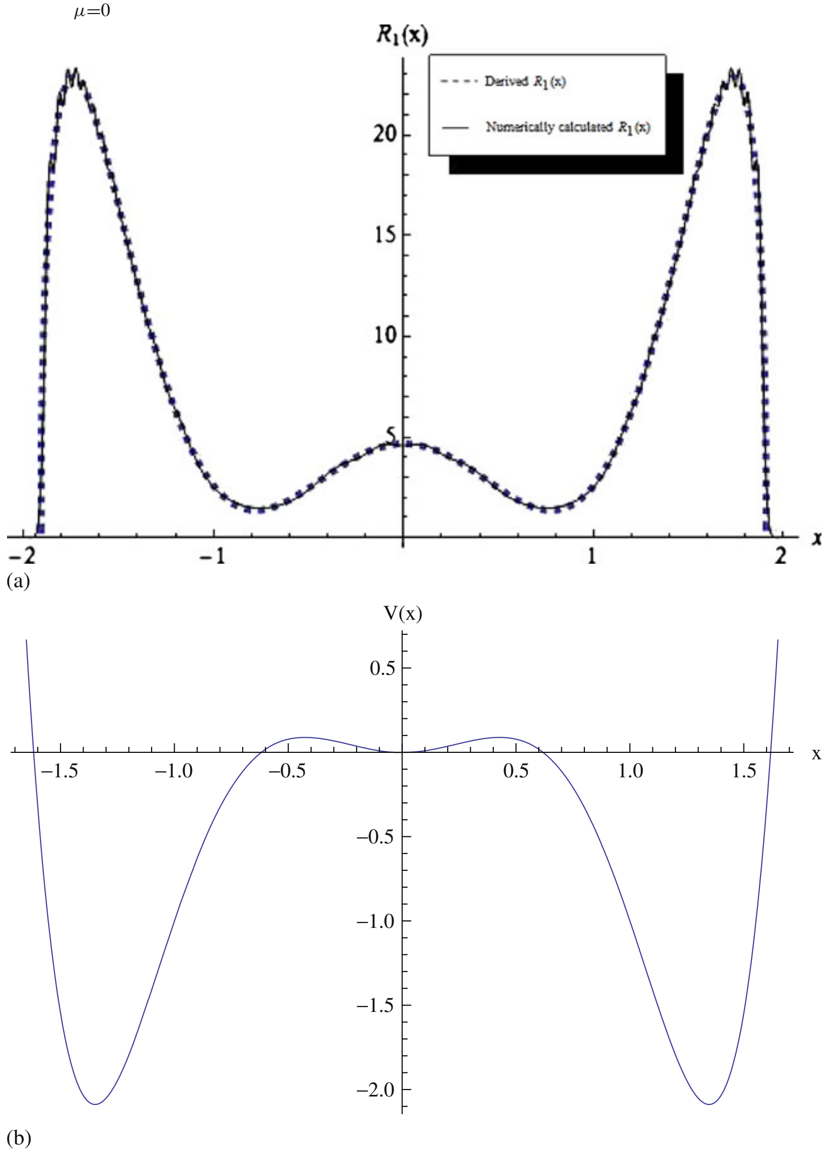

Figure 3. (**a**) Derived and actual level density plots for $a_6 = 1$, $a_4 = -3$, $a_2 = 1$, $N = 30$ with (**b**) the corresponding potential. Calculated moments are $M_2 = 62.536$, $M_4 = 164.770$.

and

$$M_6 = \sum_{\mu=0}^{N} \big(R_{\mu-2}R_{\mu-1}R_\mu + R_{\mu-1}^2 R_\mu + 2R_{\mu-1}R_\mu^2 + R_\mu^3 + 2R_{\mu-1}R_\mu R_{\mu+1} + 3R_\mu^2 R_{\mu+1} + 3R_\mu R_{\mu+1}^2 + R_{\mu+1}^3 + 2R_\mu R_{\mu+1}R_{\mu+2} + 2R_{\mu+1}^2 R_{\mu+2} + R_{\mu+1}R_{\mu+2}^2 + R_{\mu+1}R_{\mu+2}R_{\mu+3}\big). \tag{2.20}$$

The expression for M_8 and higher moments are extremely cumbersome but can be easily calculated using the aforementioned algorithm. The results for level density derived using the Dyson–Mehta method and using the method of resolvents are shown in figure 3. The corresponding potential has also been shown.

3. $d = 4$ Case

3.1 *Freud's equation*

As in the $d = 3$ case, we start with the identity

$$\int \mathrm{d}x[P_{\mu+1}(x)P_\mu(x)e^{-NV(x)}]' = 0, \tag{3.1}$$

where $V(x)$ is defined as in eq. (1.2), but with $d = 4$. Using the recursion relation for orthogonal polynomials, we get

$$\begin{aligned}\mu + 1 = NR_{\mu+1}\Bigg[&a_8\Bigg(R_{\mu+2}R_{\mu+3}\sum_{i=\mu}^{\mu+4}R_i + R_{\mu+2}^2\sum_{i=\mu}^{\mu+3}R_i + R_{\mu+2}R_{\mu+1}\sum_{i=\mu}^{\mu+2}R_i \\ &+ R_{\mu+2}R_\mu\sum_{i=\mu-1}^{\mu+1}R_i + R_{\mu+1}R_{\mu+2}\sum_{i=\mu}^{\mu+3}R_i + R_{\mu+1}^2\sum_{i=\mu}^{\mu+2}R_i \\ &+ R_\mu R_{\mu+1}\sum_{i=\mu-1}^{\mu+1}R_i + R_\mu R_{\mu+1}\sum_{i=\mu}^{\mu+2}R_i \\ &+ R_\mu R_{\mu-1}\sum_{i=\mu-2}^{\mu+1}R_i + R_\mu^2\sum_{i=\mu-1}^{\mu+1}R_i\Bigg) \\ &+ a_6\Bigg(R_{\mu+2}\sum_{i=\mu}^{\mu+3}R_i + R_{\mu+1}\sum_{i=\mu}^{\mu+2}R_i + R_\mu\sum_{i=\mu-1}^{\mu+1}R_i\Bigg) \\ &+ a_4\sum_{i=\mu-1}^{\mu+1}R_i + a_2\Bigg].\end{aligned} \tag{3.2}$$

Here we note that due to the non-linear nature of the Freud's equation, we observe oscillations in the solution for R_μ. These oscillations can be seen when the plot is divided modulo 4 into four residual bands (b_0, b_1, b_2 and b_3 in figure 4).

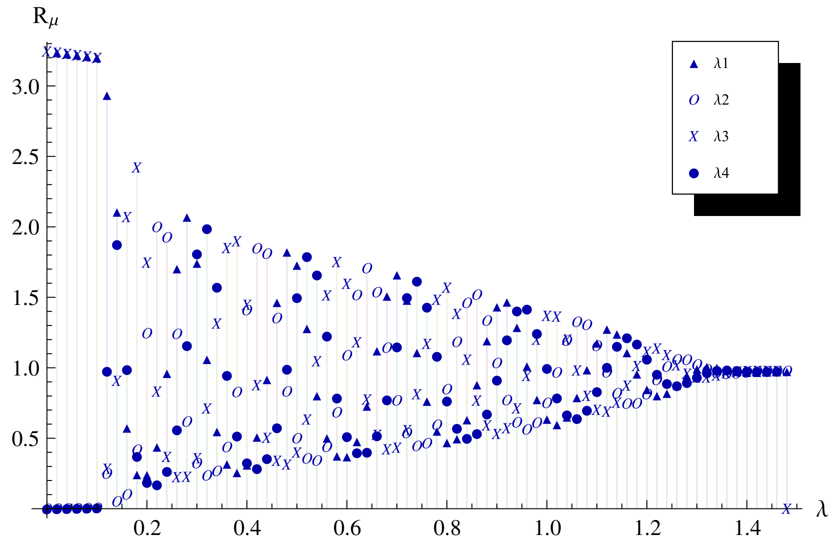

Figure 4. $d = 4$ case plot for $a_8 = 1$, $a_6 = -5$, $a_4 = 6$, $a_2 = -1$, $N = 200$.

3.2 *Level density*

Using the obtained moments and the formulation for finding level density (§2.4), we derive the function for $R_1^{(2)}(x)$ for $d = 4$ (3.3). The plot of $R_1^{(2)}(x)$ obtained using this function is compared with $R_1^{(2)}(x)$ calculated from (1.4) in figure 5. For $d = 4$, we have chosen the coefficients so that we get multiple bands in the level density.

We note that irregularities in the form of small oscillations around the expected value are seen near the peaks. This is because the numerically calculated level density is for a finite value of N. These oscillations gradually disappear as N increases.

$$\left[\frac{\pi R_1^{(2)}(x)}{N}\right]^2 = \left[\frac{a_8 M_6 + a_6 M_4 + a_4 M_2}{N} + a_2\right] + x^2 \left(a_8 x^4 + a_6 x^2 + a_4 + \frac{a_8 x^2 M_2 + a_8 M_4 + a_6 M_2}{N} - \frac{(a_8 x^6 + a_6 x^4 + a_4 x^2 + a_2)^2}{4}\right). \tag{3.3}$$

4. *d* = 5 Case

4.1 *Freud's equation*

As in the $d = 3$ case, we start with the identity

$$\int \mathrm{d}x [P_{\mu+1}(x) P_\mu(x) \mathrm{e}^{-NV(x)}]' = 0, \tag{4.1}$$

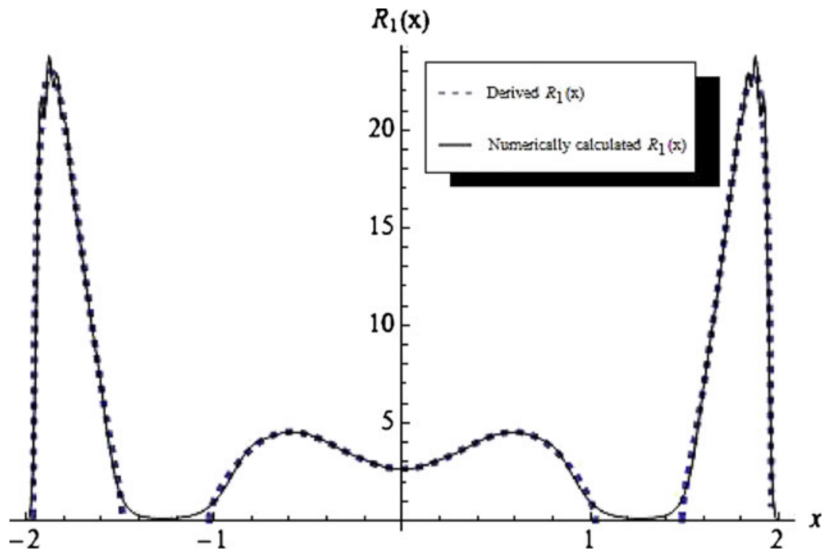

(a)

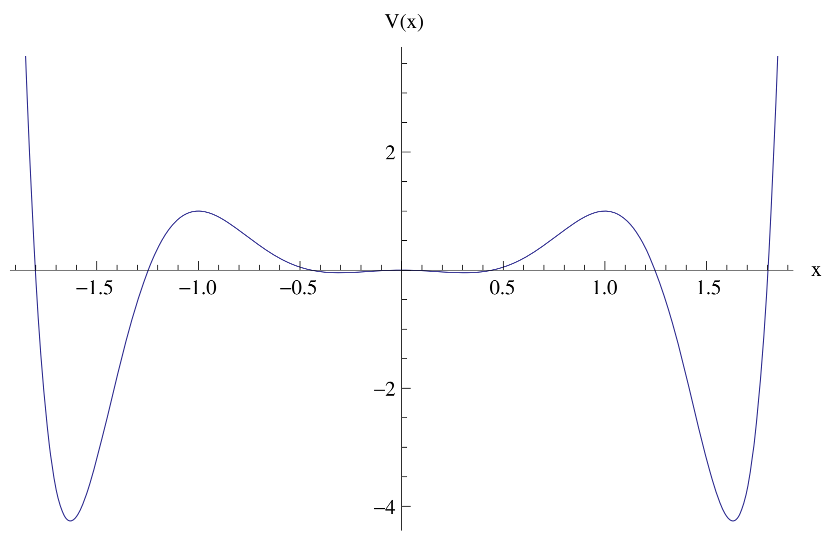

(b)

Figure 5. (**a**) Derived and actual level density plots for $d = 4$, $a_8 = 1$, $a_6 = -5$, $a_4 = 6$, $a_2 = -1$, $N = 20$ with (**b**) the corresponding potential. Calculated moments are $M_2 = 43.475$, $M_4 = 134.555$, $M_6 = 438.400$.

where $V(x)$ is defined as in eq. (1.2), but with $d = 5$. From here, one can understand that finding the Freud's equation is algorithmic in nature and we leave it to the reader to derive it explicitly. Figure 6 shows the generic plot of the R_μ function. For $d = 5$, we have chosen the coefficients so that we get multiple bands in the level density.

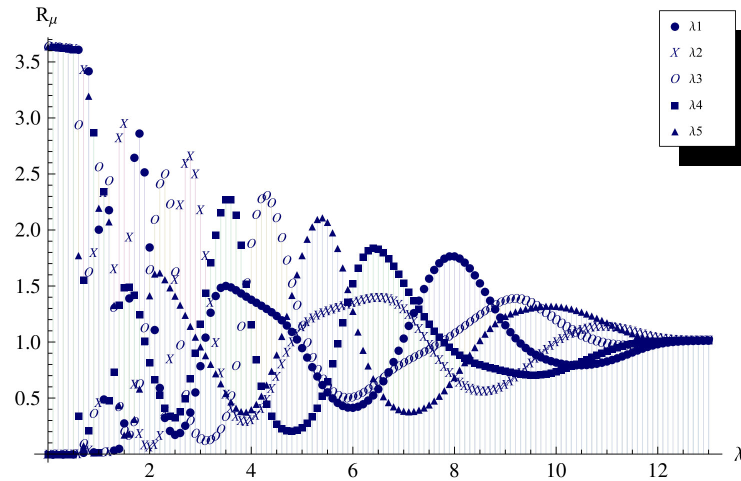

Figure 6. $d = 5$ case plot modulo 5 for $a_{10} = 10$, $a_8 = -80$, $a_6 = 210$, $a_4 = -200$, $a_2 = 48$, $N = 50$.

4.2 *Level density*

Having derived the moments M_2, M_4, M_6 and M_8 using the general formulation given in §2.4, we use the derivation provided to obtain the function for $R_1^{(2)}(x)$ for $d = 5$ (4.2). The plot of $R_1^{(2)}(x)$ obtained using this function is compared with the $R_1^{(2)}(x)$ calculated from (1.4) in figure 7.

Once again, small oscillations around the expected value are seen. This is because we are calculating $R_1^{(2)}(x)$ for a finite value of N, and these become smooth as $N \to \infty$.

$$\begin{aligned}\left[\frac{\pi R_1^{(2)}(x)}{N}\right]^2 &= \frac{a_{10}M_8 + a_8M_6 + a_6M_4 + a_4M_2}{N} \\ &+ a_2 + x^2\Bigg(a_{10}x^6 + a_8x^4 + a_6x^2 + a_4 \\ &+ \frac{a_{10}x^4M_2 + a_8x^2M_2 + a_6M_2 + a_{10}x^2M_4 + a_{10}M_6 + a_8M_4}{N}\Bigg) \\ &-\frac{x^2}{4}(a_{10}x^8 + a_8x^6 + a_6x^4 + a_4x^2 + a_2)^2. \qquad (4.2)\end{aligned}$$

5. Conclusion

In this paper, we obtain the Freud's equation for polynomials with weight function $\exp[-NV(x)]$, where $V(x) = \sum_{k=1}^{d} a_{2k}x^{2k}/2k$ is a polynomial of order $2d$. We derive the generalized Freud's equations for $d = 3$, 4 and 5. We observe limit cycle behaviour

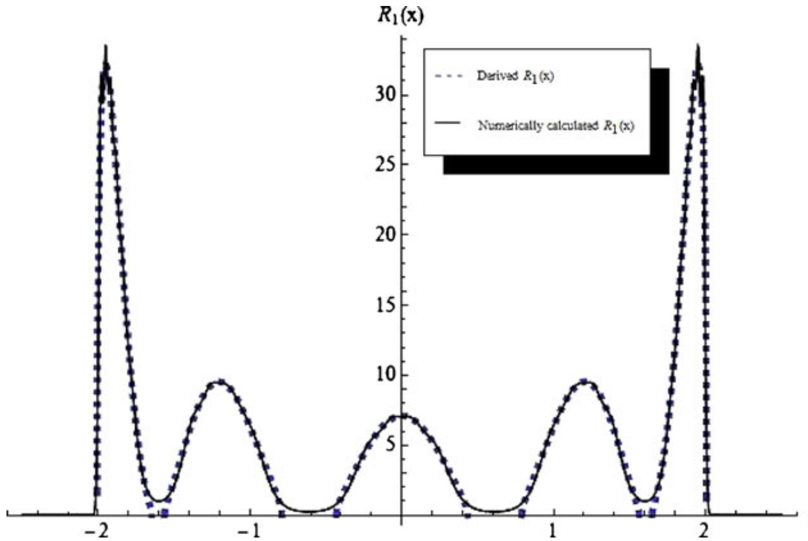

(a)

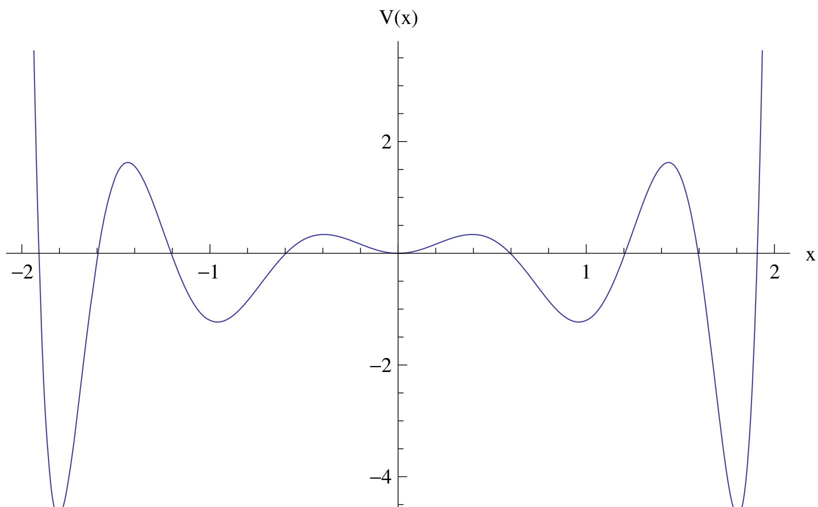

(b)

Figure 7. (**a**) Level density plot for $d = 5$, $a_5 = 1$, $a_4 = -8$, $a_3 = 21$, $a_2 = -20$, $a_1 = 4.8$, $N = 20$ with (**b**) the corresponding potential. Calculated moments are $M_2 = 43.960$, $M_4 = 136.008$, $M_6 = 460.375$, $M_8 = 1625.995$.

of R_μ. However, the apparent periodicity with period d is not as explicit as observed for the quartic case. This needs to be studied further.

We use these results and the method of resolvent to obtain the level densities of the corresponding random matrix models. However, this involves an explicit calculation of the higher moments which we calculate numerically and insert in the analytic results of the level density. It would be nice to obtain explicit results of these moments as was done for the quartic case. But we have failed in this investigation due to the complex nature of the Freud's equation.

Here, we might recall that for $d = 2$, the Freud's equation is quadratic while for higher d, it becomes cubic ($d = 3$), quartic ($d = 4$) and so on. This results in oscillations in the R_μ function and hence studying the limit cycle behaviour becomes increasingly complicated. Further investigation is needed to study these non-linear Freud's equations, specially in the context of integrability and hence the existence of Lax pairs. We wish to come back to these questions in a later publication.

References

[1] A W J Beenakker, *Rev. Mod. Phys.* **69**, 731 (1997)
[2] P Deift and D Gioev, *Int. Math. Res. Pap.* **2**, 116 (2007)
[3] P Deift and D Gioev, *Commun. Pure Appl. Math.* **60**, 867 (2007)
[4] P Deift, *Universality for mathematical and physical systems*, math-Ph/0603038
[5] G Szego, *Orthogonal polynomials* (Amer. Math. Soc., New York, NY, 1939) Vol. 23
[6] P Deift, *Courant Lect. Notes* No. 3 (Amer. Math. Society, Providence, Rhode Island, 2000)
[7] R-C Sheen, *J. Approx. Theory* **50**, 232 (1987)
[8] S Ghosh, *Skew-orthogonal polynomials and random matrix theory* (CRM Monograph Series, AMS, 2009)
[9] F J Dyson, *J. Math. Phys.* **13**, 90 (1972)
[10] F J Dyson and M L Mehta, *J. Math. Phys.* **4**, 701 (1963)
[11] M L Mehta, *Random matrices*, 3rd edn (Elsevier, The Netherlands, 2004)
[12] M L Mehta, *Matrix theory: Selected topics and useful results*, 2nd edn (Hindustan Publishing Corporation, India, 1988)
[13] P Nevai, *Siam J. Math. Anal.* **15(6)**, 1177 (1984)
[14] P A Deift, T Kriecherbauer and K T-R McLaughlin, New results for the asymptotics of orthogonal polynomials and related problems via the Lax–Levermore method, Announcement in *Proceedings of Symposia in Applied Mathematics* **54**, 87 (1998). Full text in *J. Approx. Theory* **95**, 388 (1998), under the title, New results on the equilibrium measure for logarithmic potentials in the presence of an external field
[15] P A Deift, T Kriecherbauer, K T-R McLaughlin, S Venakides and X Zhou, *Commun. Pure Appl. Math.* **52**, 1335 (1999)
[16] P A Deift, T Kriecherbauer, K T-R McLaughlin, S Venakides and X Zhou, *Commun. Pure Appl. Math.* **52**, 1491 (1999)
[17] M Plancherel and W Rotach, *Comment. Math Helv.* **1**, 227 (1929)
[18] A Stojanovic, *Math. Phys. Anal. Geom.* **3(4)**, 339 (2000)
[19] A Stojanovic, *Math. Phys. Anal. Geom.* **7(4)**, 347 (2004)
[20] A Stojanovic, Une approche par les polynmes orthogonaux pour des classes de matrices alatoires orthogonalement et symplectiquement invariantes: application l'universalité de la statistique locale des valeurs propres, Preprint, Boielefeld 00-01-006 (www.physik.uni-bielefeld.de/bibos/) (2000)
[21] G Freud, *Proc. R. Irish Acad. A* **76**, 1 (1976)
[22] S Ghosh, *Thesis* (Jawaharlal Nehru University, New Delhi, 2002) (unpublished)
[23] S Ghosh, A Pandey, S Puri and R Saha, *Phys. Rev. E* **67**, 025201 (2003)